Daily monitoring at a full-scale wastewater treatment plant reveals temporally variable micropollutant biotransformations

*Stephanie L. Rich and Damian E. Helbling**

School of Civil and Environmental Engineering, Cornell University, Ithaca, NY, 14850, USA

*Corresponding author: damian.helbling@cornell.edu, phone: +1 607 255 5146, fax: +1 607 255 9004

Keywords

stochastic microbial processes, emerging contaminants, conventional activated sludge, composite sampling, demographic shift, pharmaceuticals, organic pollutants, monohydroxylation

Abstract

Despite decades of micropollutant (MP) monitoring at wastewater treatment plants (WWTPs), we lack a fundamental understanding of the time-varying metabolic processes driving MP biotransformations. To address this knowledge gap, we collected 24-h composite samples from the influent and effluent of the conventional activated sludge (CAS) process at a WWTP over 14 consecutive days. We used liquid chromatography and high-resolution mass spectrometry (LC-HRMS) to: (i) quantify 184 MPs in the influent and effluent of the CAS process; (ii) characterize temporal dynamics of MP removal and biotransformation rate constants; and (iii) discover biotransformations linked to temporally variable MP biotransformation rate constants. We measured 120 MPs in at least one sample and 66 MPs in every sample. There were 24 MPs exhibiting temporally variable removal throughout the sampling campaign. We used hierarchical clustering analysis to reveal four temporal trends in biotransformation rate constants and found MPs with specific structural features co-located in the four clusters. We screened our HRMS acquisitions for evidence of specific biotransformations linked to structural features among the 24 MPs. Our analyses reveal that *alcohol oxidations*, *monohydroxylations at secondary or tertiary aliphatic carbons*, *dihydroxylations of vic-unsubstituted rings*, and *monohydroxylations at unsubstituted rings* are biotransformations that exhibit variability on daily timescales.

Short synopsis statement.

This research uses daily, time-proportional composite samples across a conventional activated sludge system and high-resolution mass spectrometry to reveal micropollutant biotransformations that are temporally variable on daily timescales.

Abstract art

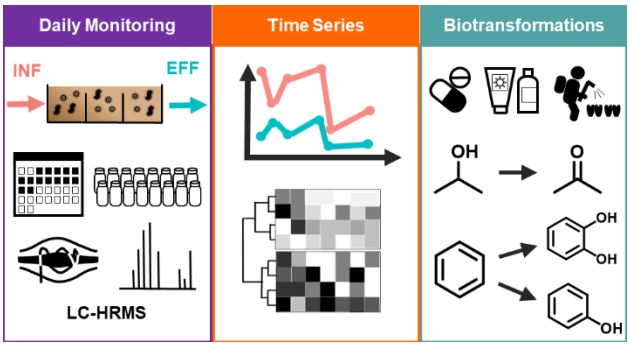

Introduction

Organic micropollutants (MPs) are an unbounded class of xenobiotics that have negative effects on water quality and exposed aquatic ecosystems.[1–3] Human exposure to MPs can also lead to a variety of negative health effects including cytotoxic and developmental effects.[4–6] Municipal wastewater treatment plants (WWTPs) play an important role in determining the fate of MPs in the environment.[7–10] One of the most important techniques for MP removal in conventional WWTPs is through aerobic biological treatment processes. For example, it is widely known that MP biotransformations are primarily catalyzed by non-specific enzymes produced by the wastewater microbial communities within conventional activated sludge (CAS) processes.[11–18] Decades of research have demonstrated that some MPs are nearly always biotransformed in CAS systems around the world (*e.g.*, ibuprofen, acetaminophen) whereas other MPs are nearly always persistent in CAS systems around the world (*e.g.*, carbamazepine, sucralose).[19,20]

Although it is useful to identify MPs that are either universally biotransformed or persistent, the majority of MPs exhibit variable rates and extent of biotransformation over time and in CAS systems around the world.[15,21,22] Variable biotransformation of MPs is often linked to process variables such as temperature,[23–25] redox environment,[26,27] solids retention time,[28,29] or the presence or absence of specific taxa within the wastewater microbial community.[30] All of these factors ultimately shape the structure and function of the wastewater microbial community and could influence the activity levels of specific microbial community functions. However, it remains unclear how changes in these process variables might change the activity level of a specific microbial community function and over what timescales changes in activity levels might be observed in a full-scale WWTP. This knowledge gap limits our ability to tune the performance of WWTPs to enhance the biotransformation of the majority of MPs.

Most previous studies investigating the variable biotransformation of MPs have utilized batch reactors seeded with wastewater microbial communities to measure the rate and extent of MP biotransformation[31–36] and to identify biotransformation products (TPs).[37,38] Data from these types of experiments have been useful for delineating biotransformation pathways[39] and for linking biotransformation rates to experimental variables such as dissolved oxygen levels[26] or the taxonomic composition of the microbial community.[40] However, there are a variety of limitations that have prevented the extrapolation of results from these types of studies to performance in full-scale systems. For example, batch reactors seeded with wastewater microbial communities represent only a snapshot of the dynamic microbial community at the time of sampling from the full-scale WWTP.[41] Further, removing the wastewater microbial community from its natural environment and placing it in a laboratory reactor is expected to result in significant shifts in both the taxonomic composition and the activity levels of specific microbial community functions.[42,43] Spiking MPs into a batch reactor can also stimulate or inhibit the activity levels of specific microbial community functions resulting in a misrepresentation of biotransformation rate constants relative to the full-scale system.[10,44–46]

We contend that novel insights on the temporal variability of MP biotransformations performed by wastewater microbial communities are best explored through daily monitoring of MP concentrations in the influent and effluent of the biological process at a full-scale WWTP. Therefore, we implemented a 14-day sampling campaign at the Ithaca Area Wastewater Treatment Facility where we collected 24-h time-proportional samples from the influent and effluent of a CAS process, concentrated each sample by means of solid-phase extraction, and used liquid chromatography coupled to high-resolution mass spectrometry (LC-HRMS) to: (i) quantify the abundance of up to 184 MPs in the influent and effluent of the full-scale CAS process daily over

a 14-day period; (ii) characterize the temporal dynamics of MP removal and biotransformation rate constants over the 14-day period; and (iii) discover specific biotransformations that are linked to temporally variable MP biotransformation rate constants. This study offers the first evaluation of the daily variability of MP biotransformations in a full-scale WWTP over a 14-day period. Our data demonstrate that some MP biotransformations can be variable on daily timescales and that MP concentration and chemical structure are driving factors in the temporal variability of MP biotransformations.

Materials and Methods

Micropollutant selection. We selected 184 MPs for target quantification in this study. The selected MPs are commonly observed in WWTPs and consist of pharmaceuticals, industrial chemicals, pesticides, human metabolites, and food additives.[9,47,48] We selected these MPs to observe population-driven chemical use patterns in the studied WWTP and to encompass a broad range of MP chemical structures. Stock solutions of all 184 MPs were prepared at 1 g L^{-1} in either LC-MS-grade methanol (OmniSolv, VWR), nanopure water (EMD Millipore), LC-MS-grade acetonitrile (Fisher Chemical), ethanol (Decon Labs), dimethyl sulfoxide (Macron Fine Chemicals) or acetone (Honeywell) and stored at -20°C. A standard mixture of all 184 MPs was created in nanopure water at 5 mg L^{-1} and stored at -20°C. A list of the 184 MPs, along with their CAS numbers, chemical formulas, and analytical parameters are provided in **Table S1** of the **Supporting Information (SI)**. Similarly, a mixture of 51 isotope-labeled internal standards (ILIS) was created in nanopure water at 5 mg L^{-1} and stored at -20°C. A list of the 51 ILISs is provided in **Table S2**.

Sampling of wastewater *in-situ*. The WWTP chosen for this study is located in Ithaca, NY and treats 6.5 MGD of raw wastewater on average for a population of approximately 30,000

inhabitants. Average daily volumetric flow rates during the 14-day sampling campaign as well as instantaneous minimum and maximum flowrates, and daily precipitation values are provided in **Figure S1**. The main biological treatment process at this WWTP consists of a CAS system with return activated sludge followed by a secondary clarifier. More information on the WWTP operational parameters during the sampling campaign are included in **Table S3.** We placed two full-size portable Teledyne ISCO 6712 autosamplers along the WWTP treatment path surrounding the CAS system, which is the WWTP unit process where we expect most MPs will be biotransformed.[12] One autosampler was placed directly upstream of the CAS at the effluent of the primary clarifier before the input of return activated sludge and the other autosampler was placed at the end of the CAS system designed with plug-flow-like hydraulics (denoted as INF and EFF respectively, see **SI Figure S2**). Daily, time-weighted composite samples were collected at each sampling location simultaneously starting from 10:00 am on November 17th and ending at 10:00 am on December 1st 2020. We chose these sampling dates to capture a demographic shift in the community caused by the outflow of students from the Cornell University and Ithaca College campuses for Thanksgiving break on Nov 26th to evaluate the effect of a population change on influent MP concentrations and wastewater microbial community functioning (we also note that 2020 was an unusual year due to the ongoing COVID-19 pandemic, but that most students were studying on campus and left town for the Thanksgiving holiday). Teflon-lined polyethylene tubing was used to draw 20 mL of wastewater every 20 min for 24 h into 1.8 L glass bottles such that the total volume of each composite sample was approximately 1.4 L. Field blanks were collected before and after wastewater sampling by running 1.4 L of nanopure water through our sample collection system. We chose to implement a simultaneous sampling method because the hydraulic retention time of the studied reactor was 7.3 h on average and our 24 h composite samples will

collect most of the MP mass traveling through the system. We retrieved composite samples from the WWTP at 10:10 am daily and prepared them in the lab within one hour of sample collection.

Preparation of wastewater samples. Wastewater samples were filtered in three different steps before preparation via solid-phase extraction (SPE). The three filtration steps included large solids removal using coffee filters (VWR), suspended solids removal using glass-fiber filters (grade GF/F, diameter 4.7 cm, pore size 0.7 μm, VWR), and finally cellulose acetate filters (diameter 4.7 cm, pore size 0.45 μm, VWR) to generate sample filtrate for SPE. One liter of sample filtrate was collected and titrated to a pH of 6.5 using dilute formic acid and spiked with 20 μL of the ILIS mixture such that each sample had an ILIS concentration of 100 ng/L before loading onto mixed-bed SPE cartridges containing 200 mg ENVI-Carb (Sigma-Aldrich), 100 mg Strata-X-AW (Phenomenex), 100 mg Strata-X-CW (Phenomenex), 150 mg Isolute ENV+ (Separtis GmbH, Germany) and 200 mg Oasis HLB (Waters) to concentrate the samples by a factor of 1000 as previously described.[49,50] We also prepared a 9-point calibration curve by spiking the mixture of 184 MPs into 1 L of nanopure water to generate standards at concentrations of 0, 1, 5, 25, 50, 100, 250, 500, and 750 ng/L. The calibration standards were likewise spiked with 20 μL of the ILIS mixture and loaded onto the mixed-bed SPE cartridges to concentrate by a factor of 1000. SPE cartridges were refrigerated at 5 °C for up to one week before elution.

Sample analysis. We adopted a previously described analytical method for MP quantification and TP identification.[9,37] Briefly, samples were measured in triplicate using reversed-phase liquid chromatography (Ultimate 3000, Thermo Scientific) coupled to high-resolution quadrupole-orbitrap mass spectrometry (QExactive, Thermo Scientific) with 30 μL injections of samples stored at 4 °C during the analysis. Samples were separated using a mobile phase gradient of LC-MS grade water (OmniSolv, 58201, solvent A) and methanol (OmniSolv, 58215, solvent B) – both

containing 0.1% (v/v) formic acid – over an XBridge C18 column (Waters, 186003021, particle size: 3.5 µm, flow rate: 0.2 mL/min, gradient properties: 0 – 5 min: 5% B, 5 – 21 min: 5% B – 95% B (linear increase), 21 – 25 min: 95% B, 25 – 30 min: 5% B). We performed full-scan MS acquisitions (100-1000 m/z, resolution 140,000) in electrospray ionization positive-negative switch mode. Data dependent MS^2 spectra were acquired at the exact masses and retention times of all target MPs and ILISs with additional MS^2 spectra collected for the TopN MS features if the inclusion list was not triggered. For absolute quantification of target analytes, we used ILIS normalized peak areas obtained with Xcalibur Quanbrowser (Thermo Scientific, Version 4.0.27.19) and a calibration series (concentration range: 0-750 µg/L after passing through SPE) with 1/x least-squares regression. Analytical parameters for each target MP and its assigned ILIS are provided in **Table S1** and **Table S2**.

Quality control. We used an in-house R script to match MS^2 fragments to candidate target MP peaks in wastewater samples (available for download at github.com/cmc493). Our workflow first converts instrument .RAW files into .mzXML files using ProteoWizard v3.0.19096, then uses the *findMsMsHR.mass* function from the R package *RMassBank*[51] to search MS^2 spectra from picked peaks for matching diagnostic fragments in our in-house database or from the highest calibration point (diagnostic fragments provided in **Table S1**). All .RAW and .mzXML files are available as data set MSV000092016 from the GNPS MassIVE repository (https://massive.ucsd.edu/ProteoSAFe/static/massive.jsp) citable under DOI: 10.25345/C5SQ8QT49. Confirmed MP detection in any sample required at least one diagnostic fragment in one of the triplicate sample measurements. For pseudo-first order rate constant estimates, concentrations greater than the highest calibration point were included and concentrations lower than the limit of quantification (LOQ) were conservatively replaced with the

value of the LOQ. The LOQ was defined as the lowest measured calibration point in our standard curve (0.001 µg/L is the lowest possible value for the LOQ). We only report concentrations of MPs where linear calibration curves consisted of at least three points and had an R^2 greater than 0.85, which addresses analytical uncertainties resulting from the matrix and analyte interference. Data quality parameters such as R^2 and LOQ for target MPs are provided in **Table S4**.

Biotransformation product analysis. We used the Eawag-Pathway Prediction System[52,53] (Eawag-PPS) with relative reasoning turned off and likelihood set to all to generate a list of 183 predicted TPs with masses greater than 100 Da for 24 select MPs that were biotransformed on every day of the sampling campaign as previously described.[38,49,54] We cross-referenced the predictions with those made by the enviPath software[55] and those contained within the sludge package of enviPath and confirmed that all possible TPs were included in our list of suspected TPs. We generated SMILES for each of the predicted TPs and used JChem for Excel (2019 version 19.26.0571) to calculate the exact mass of the $[M+H]^+$ and $[M-H]^-$ ions for each predicted TP. We then used Xcalibur Qualbrowser (Thermo Scientific, Version 4.0.27.19) to visually screen HRMS acquisitions for evidence of TP formation in the EFF dataset. We contend that TPs formed from parent MPs during the CAS process are most likely present at the EFF sampling location, therefore we prioritized TP detection in EFF samples. Evidence of TP formation includes: (i) peak areas greater than 1E5; (ii) reasonable peak shape; (iii) presence of a peak in environmental samples and absence of a peak (or peak area less than 1E4, which is a threshold for analytical noise) in blank samples; (iv) one diagnostic fragment detected in at least one triplicate measurement of a field sample; and (v) a retention time less than two minutes longer than the retention time of the parent MP. The resulting list of candidate biotransformation products was further vetted by comparing MS spectra and MS^2 fragmentation data to *in-silico* MS^2 fragments generated by the MassFrontier

194 software (ThermoScientific). MS^2 fragments were matched to predicted fragments for suspect TPs
195 using a modified version of the in-house R script described in the Quality Control section of the
196 Methods with the workflow adapted to prioritize identification of suspect TPs (available for
197 download at github.com/slr257).

198 **Data and statistical analysis.** We used MP concentrations at the INF and EFF locations to
199 estimate pseudo first-order biotransformation rate constants for MPs exhibiting removal on all 14
200 sampling days as detailed in the **SI**. We used z-score normalized first-order biotransformation rate
201 constants to compare the variability of temporal trends in MP biotransformation rate constants
202 over the 14-day period due to the wide range of the absolute values of pseudo first-order MP
203 biotransformation rate constants. Hierarchical clustering analysis was performed on the
204 normalized rate constants using Ward's agglomerative clustering method *ward.D2* in RStudio[56–
205 58] (R version 4.0.4, RStudio version 1.1.463) with the package *pheatmap*.[59] Correlation
206 coefficients (r) were calculated using Spearman's rank correlation test with the function *cor.test*
207 and significance tests were performed using two-sided, paired t-tests with the function *t.test* from
208 the R *stats* package.

209 ## Results and Discussion

210 **Quantifying MPs in INF and EFF samples.** We quantified concentrations of 152 MPs that met
211 our quality control criteria. We found 120 of the 152 MPs at concentrations above individual LOQs
212 in at least one INF or EFF sample collected during the 14-day sampling period. Of the 120 MPs
213 measured in at least one INF or EFF sample, we observed 75 in all INF samples, 72 in all EFF
214 samples, and 66 in all INF *and* EFF samples on all 14 sampling days. Additionally, field samples
215 collected before and after the sampling campaign confirmed that MPs were not accumulating in or
216 leaching from our sampling system. A summary of the quantified MPs, concentrations, and

removal percentages (%R) are provided in **Figure 1**. **Figure 1A** details the number of days each MP was observed throughout the campaign, with zero representing MPs that were *never* measured above the LOQ and 14 representing MPs that were *always* measured above the LOQ at each INF and EFF location. Most MPs at the INF location were also found at the downstream EFF location at least once with the exception of abacavir, caffeine, coumarin, levetiracetam, and meprobamate indicating consistent and complete removal of these five MPs. However, the antiviral medication abacavir and anxiolytic drug meprobamate were each observed in only one INF sample (abacavir – Nov 29th, meprobamate – Nov 24th) so we cannot say if the complete removal of these two MPs is necessarily a robust process. As shown in **Figure 1A**, the majority of quantified MPs fall into extremes of either zero or 14 days observed, with 42 and 43 MPs falling between these two extreme categories for INF and EFF respectively.

Figure 1B shows two overlaid distributions of the mean concentrations generated from triplicate measurements for the 120 target MPs measured above the LOQ in any INF or EFF sample with concentrations ranging from 0.001 – 660 µg/L on any one day. The mean and median concentrations of MPs detected at the INF location were 9.6 µg/L and 0.54 µg/L respectively. The mean and median concentrations of MPs detected at the EFF location were 2.9 µg/L and 0.32 µg/L. Summary statistics of measured concentrations for each individual MP used in the distributions in **Figure 1B** are provided in **Table S5** and **Table S6**. As shown in **Figure 1B**, there was an overall significant decrease in MP concentrations from INF to EFF samples ($p < 0.05$, t-test) indicating the expected aggregate MP removal during the CAS process, especially for MPs entering the CAS process at relatively high concentrations (5-700 µg/L). We note that although we report EFF concentrations as high as 119 µg/L (saccharin, Nov 19th), this represents the effluent of the CAS process and not the concentration of MPs released into the environment at the final WWTP

effluent; downstream unit processes at this WWTP include secondary clarification, chemical precipitation of phosphorous, disinfection, and dechlorination.

Next, we calculated %R on each day of the sampling campaign using INF and EFF concentrations ((INF-EFF)*100/INF) and evaluated the relationship between average INF concentration and average %R (**Figure 1C**). We removed MPs exhibiting sporadic %R (< 3 days) before generating **Figure 1C**, which resulted in 78 MPs for which we calculated average %R and the associated standard deviation (SD). **Figure 1C** shows average %R plotted against average log-transformed INF concentrations for these 78 MPs along with the SD represented in a color scale ranging from yellow (low SD) to red (high SD). In **Figure 1C**, we observe a weak yet significant positive relationship between average %R and average log-transformed INF concentration indicating that, in aggregate, average %R increases with increasing INF concentration ($r = 0.4$, $p < 0.05$), a phenomenon that has been observed for MPs at other WWTPs.[34] Most MPs exhibiting either very high (> 85) or very low (< 15) average %R were consistently measured as such (*i.e.*, low SD). MPs in this category are likely biotransformed via microbial community functions with stable activity levels. Conversely, MPs exhibiting less extreme average %R values (between 15-85%) exhibited more variability in measured %R (*i.e.*, high SD), demonstrating the interesting phenomenon of temporally changing activity levels for the related microbial community functions. Finally, we note that no significant associations were identified between %R and precipitation level, flow rate, suspended solids concentration, or influent and effluent BOD_5 concentrations.

Characterizing the temporal dynamics of %R. We next aimed to characterize the temporal dynamics of %R over the 14-day sampling campaign for individual MPs. To do this, we focused on the 66 MPs that were measured in all INF and EFF samples on all 14 days of the sampling campaign. We then narrowed that list to 35 MPs that exhibit positive %R on all 14 days of the

sampling campaign; the other 31 MPs exhibit negative or zero %R on at least one of the sampling days which we attribute to formation during activated sludge treatment (*e.g.*, back-transformation of human metabolites to parent MPs)[44,60,61], the measured MP being a biotransformation product itself (*e.g.*, metolachlor ESA), or limited transformation resulting in near-zero %R on most days with analytical uncertainty yielding %R estimates in the range of ±15%. Temporal profiles of INF, EFF, and %R for three representative MPs that meet these criteria are provided in **Figure 2.** Temporal profiles for all 35 MPs are provided in **Figure S3**.

These data demonstrate that individual MPs can exhibit highly variable %R on daily timescales within a single WWTP. For example, propranolol exhibits a sudden drop in %R on one sampling day (Nov 25th, day before Thanksgiving holiday) before returning to pre-Thanksgiving holiday levels (**Figure 2B**). Gabapentin exhibits large daily increases in %R over the first four days of the sampling campaign before leveling off at a more consistent level during the latter seven days of the sampling campaign (**Figure 2C**). This important observation of highly variable %R on daily timescales within a single WWTP has not been clearly demonstrated in previous literature (although highly variable MP concentrations in WWTP effluents has been reported)[62] and has several practical implications. First, these data confirm that a single 24-h composite sample is insufficient to determine the %R of an individual MP; rather, a time-series of daily composite samples are needed to fully capture the temporal variability of %R within a single WWTP. Second, the temporal variability itself is notable because it suggests there are factors that change on daily (or hourly) timescales that influence the activity levels of microbial community functions involved in MP biotransformations at a full-scale WWTP.

Next, we tested whether the demographic shift in the community due to the Thanksgiving holiday break resulted in significant changes in aggregate INF concentrations or %R for the 35

MPs. We compared the distributions of INF concentrations and %R for the 35 MPs from the five days before the Thanksgiving holiday (Nov 20^{th} – 25^{th}) to the five days after the Thanksgiving holiday (Nov 26^{th} – Dec 1^{st}). We observed significant decreases in INF concentrations ($p < 0.05$, t-test) and %R ($p < 0.01$, t-test) for the 35 MPs in the five days after the Thanksgiving holiday, indicating that the demographic shift had effects on INF concentrations and %R. Previous studies have demonstrated that a sudden demographic shift can be associated with the expected decreases (and sometimes increases) in MP concentrations in WWTPs.[63] However, our data indicate this type of demographic shift can likewise influence the activity levels of microbial community functions involved in MP biotransformations at a full-scale WWTP.

Although we observed significant decreases in *aggregate* INF concentrations and %R in the five days after Thanksgiving break, it is also clear from the data in **Figure 2** and **Figure S3** that changes in INF are not always associated with changes in %R among individual MPs. To test the relationship between INF concentrations and %R among the 35 individual MPs, we used the SD values of %R to evaluate the extent of variability of %R and Spearman correlations between INF concentrations and %R to identify significant associations. We identified three major types of relationships between INF concentrations and %R based on these metrics. First, we identified ten MPs that did not exhibit variable %R over the fourteen-day sampling campaign (SD < 5%) despite changes in INF concentrations. These include caffeine (**Figure 2A**) and nine other MPs listed in **Table S7**. Examination of the temporal profiles of %R for these MPs indicates that they are all nearly completely removed on every day of the sampling campaign. Therefore, there is no measurable change in the activity levels of the microbial community functions involved in the biotransformation of these MPs. Second, we identified eight MPs that exhibit variable %R (SD > 5%) and a positive and significant association between INF concentration and %R ($r > 0.55$, $p <$

0.05). These include propranolol (**Figure 2B**) and seven other MPs listed in **Table S7**. These associations suggest that INF concentrations may have an effect on the activity levels of the microbial community functions involved in the biotransformation of these MPs. Third, we identified sixteen MPs exhibiting variable %R (SD > 5%) with no significant association between INF concentration and %R ($-0.55 < r < 0.55$, $p > 0.05$). These include gabapentin (**Figure 2C**) and 15 other MPs listed in **Table S7**. These sixteen MPs are of particular interest for this study because they exhibit temporal variability in %R on daily timescales, but the variability is not associated with changes in INF concentration. Therefore, we conclude that the activity levels of the microbial community functions involved in the biotransformation of these MPs are changing in response to other, unknown factors. Finally, we must note that acesulfame exhibits variable %R (SD > 5%) and a negative and significant association between INF concentration and %R ($r < -0.55$, $p < 0.05$). Variable removal of acesulfame in WWTPs has been previously reported and has been linked to adaptation of the microbial community to continuous exposure to acesulfame.[22] The negative and significant association observed here was unique to acesulfame and has not been previously reported for other MPs. Because this unique behavior could not be generalized to a broader group of MPs, we do not include acesulfame in the following analyses.

Characterizing the temporal dynamics of MP biotransformation rate constants. We next aimed to characterize the temporal dynamics of MP biotransformation rate constants over the 14-day sampling campaign for individual MPs. Biotransformation rate constants are a complementary metric to %R that account for large differences in INF concentrations among MPs while incorporating daily changes in hydraulic retention time. We used **Equation S1** to estimate pseudo first-order rate constants on each day of the sampling campaign for the 24 MPs that exhibit variable %R (SD > 5%) as described in the preceding section. The estimated average rate constants range

from 0.02 to 24 d^{-1} with a median value of 2.8 d^{-1}. Mean values of the rate constants for each of the 24 MPs along with their respective maximum, minimum, and coefficient of variation (CoV) across the 14-day sampling campaign are provided in **Table S8**. Metalaxyl, metaxalone, famotidine, and dimethyl phthalate exhibited the most variable biotransformations rate constants (CoV > 0.62) and DEET, emtricitabine, propranolol, and flucytosine exhibited the least variable biotransformation rate constants (0.15 < CoV < 0.26).

To evaluate whether groups of MPs exhibit characteristic patterns of variability among their biotransformation rate constants, we used z-score normalization (to eliminate the effects of the magnitudes of the rate constants) and hierarchical clustering to generate the clustered heatmap shown in **Figure 3**. This analysis revealed four clusters of MPs that exhibit correlated patterns of variability among their biotransformation rate constants. Boxplots of actual rate constant values by cluster per day are provided in **Figure S4**. The eight MPs labeled with red text in **Figure 3** represent those that exhibit positive and significant associations between INF concentration and %R as described in the preceding section. It is interesting to note that all eight of these MPs are contained within cluster 1 and cluster 2, suggesting that INF concentrations may be an important factor controlling the activity level of the microbial community functions involved in the biotransformation of the MPs in these two clusters. MPs in cluster 3 are characterized by their maximum biotransformation rate constants on Nov 21st and a general decreasing trend in rate constant magnitudes after this date (evidenced by the shading of the heat map in **Figure 3** and the data presented in **Figure S4**). MPs in cluster 4 are characterized by steadily increasing rate constants over the 14-day sampling campaign (evidenced by the shading of the heat map in **Figure 3** and the data presented in **Figure S4**). All twelve of the MPs contained in cluster 3 and cluster 4 are among those that exhibit no significant association between INF concentration and %R,

suggesting that the activity levels of the microbial community functions involved in the biotransformation of the MPs in these two clusters are changing in response to other, unknown factors. We note that changing activity levels could be the result of shifts in microbial community structure or shifts in the expression levels of genes that encode for the associated catalytic enzymes.[64,65] The specific taxa and catalytic enzymes involved in the observed MP biotransformations are unknown, but literature data demonstrate that the core structure of wastewater microbial communities is stable over weekly or even monthly timescales,[66] whereas gene expression levels can vary over hourly or daily timescales.[67] Therefore, it is likely that the changes in activity levels are the result of either changes in the composition of satellite taxa around the core structure or changing gene expression levels resulting from environmental or stochastic processes.[68] Because the specific taxa and catalytic enzymes involved in the observed MP biotransformations are unknown, this cannot be explicitly tested but is motivation for future research.

We hypothesize that chemical structure could be a factor that explains the patterns of variability among the biotransformation rate constants of the MPs contained in the four clusters revealed in **Figure 3**. Under this hypothesis, clusters of MPs containing common labile functional groups would exhibit correlated patterns of temporally variable biotransformations based on changing activity levels of related microbial community functions. To test this hypothesis, we used the Eawag-PPS to identify the biotransformation rules (btrules) triggered by each of the 24 MPs contained in **Figure 3**. This analysis revealed 36 unique btrules triggered by all 24 MPs, with nine btrules that represent four broad categories of biotransformations predicted most consistently. A summary of this analysis is presented in **Figure 4A**, where we report the number of times each of the nine btrules was triggered by the MPs contained in each of the four clusters.

We found that the five MPs in cluster 1 primarily contain functional groups that support both *alcohol oxidations* (bt0001, bt0002) and *monohydroxylations at secondary or tertiary aliphatic carbons* (bt0241, bt0242). Conversely, the seven MPs in cluster 2 contain functional groups that support both *dihydroxylations of vic-unsubstituted rings* (bt0005) and *monohydroxylations at unsubstituted rings* (bt0011, bt0012, bt0013, bt0014). The observation that each cluster of MPs contains functional groups in common supports our hypothesis. Further, because we previously noted that most of the MPs contained in cluster 1 and cluster 2 exhibit positive and significant associations between INF concentration and %R, these data suggest that the activity levels of these microbial community functions may be influenced by INF concentrations. The four MPs in cluster 3 primarily contain functional groups that support *monohydroxylations at unsubstituted rings* (bt0011, bt0012, bt0013, bt0014) and the eight MPs in cluster 4 contain functional groups that support *monohydroxylations at secondary or tertiary aliphatic carbons* (bt0241, bt0242). These observations likewise support our hypothesis, and our previous observation that these MPs exhibit no significant association between INF concentration and %R suggests that the activity levels of these microbial community functions for these MPs may be changing in response to other, unknown factors.

Discovering specific biotransformations linked to variable rate constants. We finally aimed to provide additional support to our hypothesis by screening the EFF samples for evidence of TPs formed from specific biotransformations noted for each of the four MP clusters. We used the Eawag-PPS predictions to screen the EFF samples for a total of 183 TPs. We found evidence of 37 TPs formed from 18 of the 24 MPs in at least one EFF sample. A summary of detected TPs along with their respective SMILES, chemical formula, extracted mass, retention times, diagnostic fragments, and associated btrules is provided in **Table S9** and definitions of associated btrules are

provided in **Table S10**. All 37 of the TPs are identified at confidence level 2 or 3 according to Schymanski et al.[69] We also present an accounting of the TPs that were detected resulting from the nine btrules most commonly triggered by the 24 MPs in **Figure 4B**. The data in **Figure 4B** demonstrate that we found evidence of TPs representing all four broad categories biotransformations (or microbial community functions) sporadically across the four MP clusters. Although we did find evidence of some of the expected biotransformations in some of the clusters (*e.g.*, four TPs resulting from *monohydroxylations at secondary or tertiary aliphatic carbons* for MPs contained in cluster 4), this analysis does not provide unequivocal evidence in support of our hypothesis.

It is worth discussing some of the limitations of our approach to TP analysis that may confound our ability to definitively identify evidence of the expected biotransformations. First, we restricted our analysis to only those TPs predicted by the Eawag-PPS. Although this is one of the most robust tools available to predict biotransformations of MPs performed by wastewater microbial communities,[70] it is not necessarily comprehensive and recent studies have reported biotransformations performed by wastewater microbial communities that are not predicted by the Eawag-PPS.[37,39,71] This limitation restricts our ability to account for likely biotransformations (**Figure 4A**) and our ability to screen for TPs in the EFF samples (**Figure 4B**). Second, it is possible that some of the predicted TPs cannot be detected using our analytical method that was optimized for the quantification of the 184 MPs of interest within a certain mass range and that are captured using our SPE method. Further, our stringent criteria for analytical data supporting TP identification may have filtered out some TPs that actually were present. These factors highlight the limitations of HRMS as a tool for identifying TPs in complex matrices. Third, most studies that report on MP biotransformations are conducted in batch studies in which the MP of interest is

spiked into a wastewater microbial community. Whereas other studies have screened for TPs in wastewater effluent,[72] our study is one of the first to try to identify TPs *in-situ* without prior knowledge of expected TPs from batch experiments, which limits our ability to leverage experimental tools to facilitate TP identification (*e.g.*, temporal trend analysis). Nevertheless, this approach was essential to capture the temporal dynamics and limit the effects of microbial community harvesting and MP spiking in batch reactors. Finally, it is likely that some of the expected biotransformations occurred as a relatively rapid first step along a biotransformation pathway. We observed the first step as the disappearance of the MP, but the first-generation TP may not have been formed to a measurable extent before it was subsequently biotransformed. These limitations point to the need for improved prediction of biotransformations occurring during wastewater treatment and analytical methods for TP detection in wastewater effluents.

Environmental implications. The primary goal of this study was to discover the extent of the temporal variability of MP biotransformations performed by wastewater microbial communities. Our data demonstrate that some MPs exhibit variable biotransformations (as evidenced by %R and biotransformation rate constants) over daily timescales. The MPs that exhibited the most variable %R and biotransformation rate constants were metalaxyl, metaxalone, famotidine, and dimethyl phthalate. Variable biotransformation was significantly and positively associated with INF concentrations for eight MPs including propranolol, clindamycin, ritalinic acid, benzotriazole, lidocaine, gemfibrozil, flucytosine, and metalaxyl. These novel observations suggest a potential link between INF concentrations and the activity levels of the microbial community functions involved in the biotransformation of these MPs. However, variable biotransformation was not associated with INF concentrations for most MPs, and we suggest that the activity levels of the microbial community functions involved in the biotransformation of those MPs are changing in

response to other, unknown factors. Our analysis of chemical structure and likely biotransformations suggests that *alcohol oxidations*, *monohydroxylations at secondary or tertiary aliphatic carbons*, *dihydroxylations of vic-unsubstituted rings*, and *monohydroxylations at unsubstituted rings* are biotransformations that may exhibit variable activity levels on daily timescales. These biotransformations are catalyzed by enzymes in the broad classes of dehydrogenases (EC 1.1.-.-), monooxygenases (EC 1.14.-.-), and dioxygenases (EC 1.14.-.-) and are expected to be co-metabolic.[27]

There is a need to better understand the factors that control the removal of MPs during wastewater treatment. Our data demonstrate that some MPs are always removed (*e.g.*, acetaminophen, caffeine, coumarin) whereas other MPs are always persistent (*e.g.*, sucralose, carbamazepine). These observations agree with previous data reported from WWTPs from around the world.[61,73] However, most MPs are removed to variable extents across WWTPs and, as our data demonstrate, within a single WWTP over daily timescales. We argue that this latter group of MPs represent an opportunity to improve the performance of WWTPs for removing MPs. Our data suggest this group of MPs *can* be completely removed during conventional wastewater treatment; we only need to understand the causal factors that result in increased activity levels of the associated biotransformations. This study provides a step forward toward that goal.

Supporting Information

list of target micropollutants; details on flow conditions and operational parameters at wastewater treatment plant; analytical information on detected MPs; pseudo-first order rate constant equation; summary statistics of detected MP; temporal profiles of INF and EFF concentrations and %R; binned MPs according to correlation between INF concentration and %R; summary statistics of MP rate constants over 14-day sampling period; boxplots of rate constants grouped by clusters

from Figure 3; analytical information for detected TPs; definitions of biotransformation rules (btrules); R code used for generating figures can be found here: https://github.com/slr257.

Acknowledgments

We thank Jose Lozano and the team of operators at the Ithaca Area Wastewater Treatment Facility for access to the treatment plant and Kevin Sarmiento for technical help during the sampling campaign. This work was supported by the United States National Science Foundation, United States (CBET-1748982).

Figure Captions

Figure 1: [A] Histogram of MPs observed N times (N = labels above the bars) during the sampling campaign at each INF (red) and EFF (blue) location (y-axis) binned into groups ranging from 0-14 days detected (x-axis). **[B]** Histogram of 120 target MP concentrations in samples (y-axis) at INF and EFF locations with **30** bins ranging from 10^{-3} to 10^{3} µg/L (x-axis). **[C]** Relationship between average %R, INF concentration, and standard deviation of %R (SD) for the 78 MPs that exhibited removal on at least three days of the sampling campaign. Red shading refers to MPs with high SD, and yellow shading refers to MPs with low SD with respect to %R.

Figure 2: Temporal concentration profiles in ng/L at INF (red) and EFF (blue) locations plotted with calculated %R for all 14 days of the sampling campaign for caffeine [A], propranolol [B], and gabapentin [C].

Figure 3: Heatmap of z-score normalized pseudo-first-order biotransformation rate constant estimates for 24 MPs that were biotransformed on all 14 days of the sampling campaign with temporally variable %R where zero represents the mean biotransformation rate constant (white) and red and blue cells represent higher and lower than average biotransformation rate constants respectively. The eight MPs exhibiting positive and significant associations between %R and INF concentration ($r > 0.55$, $p < 0.05$) are highlighted with red text. There are four distinct clusters characterized by events with high increase or decrease in biotransformation rate constants on one sampling day; we note that the number of clusters was determined using the sum of squared differences.

Figure 4: Stacked barplots showing counts of the nine predicted btrules [A] representing the four broad biotransformation trends in Figure 3 compared to observed btrules [B] for each of the four clusters. Each hue represents a reaction type, where purples are alcohol oxidations, red is dihydroxylations of vic-unsubstituted rings, blues are monohydroxylations at unsubstituted rings, and oranges are monohydroxylations at secondary or tertiary aliphatic carbons. Definitions of biotransformation rules (btrules) are provided in Table S10 of the Supporting Information. Note: some predicted TPs may not be detectable with the analytical method used in this project.

References

(1) Schwarzenbach, R.; Escher, B. I.; Fenner, K.; Hofstetter, T. B.; Johnson, C. A.; Von Gunten, U.; Wehrli, B. The Challenge of Micropollutants. *Science.* **2006**, *313*, 1072–1077.

(2) Tian, Z.; Zhao, H.; Peter, K. T.; Gonzalez, M.; Wetzel, J.; Wu, C.; Hu, X.; Prat, J.; Mudrock, E.; Hettinger, R.; Cortina, A. E.; Biswas, R. G.; Kock, F. V. C.; Soong, R.; Jenne, A.; Du, B.; Hou, F.; He, H.; Lundeen, R.; Gilbreath, A.; Sutton, R.; Scholz, N. L.; Davis, J. W.; Dodd, M. C.; Simpson, A.; McIntyre, J. K.; Kolodziej, E. P. A Ubiquitous Tire Rubber–Derived Chemical Induces Acute Mortality in Coho Salmon. *Science.* **2021**, *371* (6525), 185–189. https://doi.org/10.1126/science.abd6951.

(3) von Wyl, M.; Könemann, S.; vom Berg, C. Different Developmental Insecticide Exposure Windows Trigger Distinct Locomotor Phenotypes in the Early Life Stages of Zebrafish. *Chemosphere* **2023**, *317*, 137874. https://doi.org/10.1016/j.chemosphere.2023.137874.

(4) Colborn, T.; Vom Saal, F. S.; Soto, A. M. Developmental Effects of Endocrine-Disrupting Chemicals in Wildlife and Humans Convincing Evidence Exists That a Variety Of. *Environ. Health Perspect.* **1993**, *101* (5), 378–384.

(5) Paquette, A. G.; Macdonald, J.; Lapehn, S.; Bammler, T.; Kruger, L.; Day, D. B.; Price, N. D.; Loftus, C.; Kannan, K.; Marsit, C.; Mason, W. A.; Bush, N. R.; Lewinn, K. Z.; Enquobahrie, D. A.; Prasad, B.; Karr, C. J.; Sathyanarayana, S. A Comprehensive Assessment of Associations between Prenatal Phthalate Exposure and the Placental Transcriptomic Landscape. *Environ. Health Perspect.* **2021**, *129* (9). https://doi.org/10.1289/EHP8973.

(6) Tang, J. Y. M.; McCarty, S.; Glenn, E.; Neale, P. A.; Warne, M. S. J.; Escher, B. I. Mixture Effects of Organic Micropollutants Present in Water: Towards the Development of Effect-Based Water Quality Trigger Values for Baseline Toxicity. *Water Res.* **2013**, *47* (10), 3300–3314. https://doi.org/10.1016/j.watres.2013.03.011.

(7) Eggen, R. I. L.; Hollender, J.; Joss, A.; Schärer, M.; Stamm, C. Reducing the Discharge of Micropollutants in the Aquatic Environment: The Benefits of Upgrading Wastewater Treatment Plants. *Environ. Sci. Technol.* **2014**, *48* (14), 7683–7689. https://doi.org/10.1021/es500907n.

(8) Chiaia-Hernández, A.; Günthardt, B.; Frey, M.; Hollender, J. Unravelling Contaminants in the Anthropocene Using Statistical Analysis of Liquid Chromatography–High-Resolution Mass Spectrometry Nontarget Screening Data Recorded in Lake Sediments. *Environ. Sci. Technol.* **2017**, *51* (21), 12547–12556. https://doi.org/10.1021/acs.est.7b03357.

(9) Carpenter, C. M. G.; Helbling, D. E. Widespread Micropollutant Monitoring in the Hudson River Estuary Reveals Spatiotemporal Micropollutant Clusters and Their Sources. *Environ. Sci. Technol.* **2018**, *52* (11), 6187–6196. https://doi.org/10.1021/acs.est.8b00945.

(10) Zhi, H.; Mianecki, A. L.; Kolpin, D. W.; Klaper, R. D.; Iwanowicz, L. R.; LeFevre, G. H. Tandem Field and Laboratory Approaches to Quantify Attenuation Mechanisms of Pharmaceutical and Pharmaceutical Transformation Products in a Wastewater Effluent-Dominated Stream. *Water Res.* **2021**, *203*. https://doi.org/10.1016/j.watres.2021.117537.

(11) Svendsen, S. B.; El-taliawy, H.; Carvalho, P. N.; Bester, K. Concentration Dependent Degradation of Pharmaceuticals in WWTP Effluent by Biofilm Reactors. *Water Res.* **2020**, *186*, 116389. https://doi.org/10.1016/J.WATRES.2020.116389.

(12) Carballa, M.; Omil, F.; Lema, J. M.; Llompart, M.; García-Jares, C.; Rodríguez, I.; Gómez, M.; Ternes, T. Behavior of Pharmaceuticals, Cosmetics and Hormones in a Sewage

Treatment Plant. *Water Res.* **2004**, *38* (12), 2918–2926. https://doi.org/10.1016/J.WATRES.2004.03.029.

(13) Ahmed, M. B.; Zhou, J. L.; Ngo, H. H.; Guo, W.; Thomaidis, N. S.; Xu, J. Progress in the Biological and Chemical Treatment Technologies for Emerging Contaminant Removal from Wastewater: A Critical Review. *J. Hazard. Mater.* **2017**, *323*, 274–298. https://doi.org/10.1016/J.JHAZMAT.2016.04.045.

(14) Fischer, K.; Majewsky, M. Cometabolic Degradation of Organic Wastewater Micropollutants by Activated Sludge and Sludge-Inherent Microorganisms. *Appl. Microbiol. Biotechnol.* **2014**, *98* (15), 6583–6597. https://doi.org/10.1007/s00253-014-5826-0.

(15) Alvarino, T.; Lema, J.; Omil, F.; Suárez, S. Trends in Organic Micropollutants Removal in Secondary Treatment of Sewage. *Rev. Environ. Sci. Biotechnol.* **2018**, *17* (3), 447–469. https://doi.org/10.1007/s11157-018-9472-3.

(16) Burzio, C.; Nivert, E.; Mattsson, A.; Svahn, O.; Persson, F.; Modin, O.; Wilén, B. M. Removal of Organic Micropollutants in the Biological Units of a Swedish Wastewater Treatment Plant. *IOP Conf. Ser. Mater. Sci. Eng.* **2021**, *1209* (1), 012016. https://doi.org/10.1088/1757-899X/1209/1/012016.

(17) Zhang, Y.; Geißen, S. U.; Gal, C. Carbamazepine and Diclofenac: Removal in Wastewater Treatment Plants and Occurrence in Water Bodies. *Chemosphere* **2008**, *73* (8), 1151–1161. https://doi.org/10.1016/J.CHEMOSPHERE.2008.07.086.

(18) Ternes, T. A.; Joss, A.; Siegrist, H. Scrutinizing Pharmaceuticals and Personal Care Products in Wastewater Treatment. *Environ. Sci. Technol.* **2004**, *38* (20), 392A-399A. https://doi.org/10.1021/es040639t.

(19) Oulton, R. L.; Kohn, T.; Cwiertny, D. M. Pharmaceuticals and Personal Care Products in Effluent Matrices: A Survey of Transformation and Removal during Wastewater Treatment and Implications for Wastewater Management. *Journal of Environmental Monitoring*. November 2010, pp 1956–1978. https://doi.org/10.1039/c0em00068j.

(20) Luo, Y.; Guo, W.; Ngo, H. H.; Nghiem, L. D.; Hai, F. I.; Zhang, J.; Liang, S.; Wang, X. C. A Review on the Occurrence of Micropollutants in the Aquatic Environment and Their Fate and Removal during Wastewater Treatment. *Sci. Total Environ.* **2014**, *473–474*, 619–641. https://doi.org/10.1016/j.scitotenv.2013.12.065.

(21) Choubert, J.-M.; Martin Ruel, S.; Miege, C.; Coquery, M. Rethinking Micropollutant Removal Assessment Methods for Wastewater Treatment Plants – How to Get More Robust Data? *Water Sci. Technol.* **2017**, *75* (12), 2964–2972. https://doi.org/10.2166/wst.2017.181.

(22) Kahl, S.; Kleinsteuber, S.; Nivala, J.; Van Afferden, M.; Reemtsma, T. Emerging Biodegradation of the Previously Persistent Artificial Sweetener Acesulfame in Biological Wastewater Treatment. *Environ. Sci. Technol.* **2018**, *52* (5), 2717–2725. https://doi.org/10.1021/acs.est.7b05619.

(23) Castiglioni, S.; Bagnati, R.; Fanelli, R.; Pomati, F.; Calamari, D.; Zuccato, E. Removal of Pharmaceuticals in Sewage Treatment Plants in Italy. *Environ. Sci. Technol.* **2006**, *40* (1), 357–363. https://doi.org/10.1021/es050991m.

(24) M. Vieno, N.; Tuhkanen, T.; Kronberg, L. Seasonal Variation in the Occurrence of Pharmaceuticals in Effluents from a Sewage Treatment Plant and in the Recipient Water. *Environ. Sci. Technol.* **2005**, *39* (21), 8220–8226. https://doi.org/10.1021/es051124k.

(25) Di Marcantonio, C.; Chiavola, A.; Dossi, S.; Cecchini, G.; Leoni, S.; Frugis, A.; Spizzirri, M.; Boni, M. R. Occurrence, Seasonal Variations and Removal of Organic Micropollutants

in 76 Wastewater Treatment Plants. *Process Saf. Environ. Prot.* **2020**, *141*, 61–72. https://doi.org/10.1016/j.psep.2020.05.032.
(26) Stadler, L. B.; Love, N. G. Oxygen Half-Saturation Constants for Pharmaceuticals in Activated Sludge and Microbial Community Activity under Varied Oxygen Levels. *Environ. Sci. Technol.* **2019**, *53* (4), 1918–1927. https://doi.org/10.1021/acs.est.8b06051.
(27) Kennes-Veiga, D. M.; Gónzalez-Gil, L.; Carballa, M.; Lema, J. M. Enzymatic Cometabolic Biotransformation of Organic Micropollutants in Wastewater Treatment Plants: A Review. *Bioresour. Technol.* **2022**, *344*, 126291. https://doi.org/10.1016/J.BIORTECH.2021.126291.
(28) Achermann, S.; Falås, P.; Joss, A.; Mansfeldt, C. B.; Men, Y.; Vogler, B.; Fenner, K. Trends in Micropollutant Biotransformation along a Solids Retention Time Gradient. *Environ. Sci. Technol.* **2018**, *52* (20), 11601–11611. https://doi.org/10.1021/acs.est.8b02763.
(29) Falås, P.; Wick, A.; Castronovo, S.; Habermacher, J.; Ternes, T. A.; Joss, A. Tracing the Limits of Organic Micropollutant Removal in Biological Wastewater Treatment. *Water Res.* **2016**, *95*, 240–249. https://doi.org/10.1016/j.watres.2016.03.009.
(30) Zhou, N. A.; Lutovsky, A. C.; Andaker, G. L.; Gough, H. L.; Ferguson, J. F. Cultivation and Characterization of Bacterial Isolates Capable of Degrading Pharmaceutical and Personal Care Products for Improved Removal in Activated Sludge Wastewater Treatment. *Biodegradation* **2013**, *24* (6), 813–827. https://doi.org/10.1007/s10532-013-9630-9.
(31) Helbling, D. E.; Hollender, J.; Kohler, H. P. E.; Fenner, K. Structure-Based Interpretation of Biotransformation Pathways of Amide-Containing Compounds in Sludge-Seeded Bioreactors. *Environ. Sci. Technol.* **2010**, *44* (17), 6628–6635. https://doi.org/10.1021/es101035b.
(32) Helbling, D. E.; Hollender, J.; Kohler, H. P. E.; Singer, H.; Fenner, K. High-Throughput Identification of Microbial Transformation Products of Organic Micropollutants. *Environ. Sci. Technol.* **2010**, *44* (17), 6621–6627. https://doi.org/10.1021/es100970m.
(33) Fenner, K.; Screpanti, C.; Renold, P.; Rouchdi, M.; Vogler, B.; Rich, S. Comparison of Small Molecule Biotransformation Half-Lives between Activated Sludge and Soil: Opportunities for Read-Across? *Environ. Sci. Technol.* **2020**, *54* (6), 3148–3158. https://doi.org/10.1021/acs.est.9b05104.
(34) van Bergen, T. J. H. M.; Rios-Miguel, A. B.; Nolte, T. M.; Ragas, A. M. J.; van Zelm, R.; Graumans, M.; Scheepers, P. T. J.; Jetten, M. S. M.; Hendriks, A. J.; Welte, C. U. Do Initial Concentration and Activated Sludge Seasonality Affect Pharmaceutical Biotransformation Rate Constants? *Appl. Microbiol. Biotechnol.* **2021**, *105* (16), 6515–6527. https://doi.org/10.1007/s00253-021-11475-9.
(35) Helbling, D. E.; Johnson, D. R.; Honti, M.; Fenner, K. Micropollutant Biotransformation Kinetics Associate with WWTP Process Parameters and Microbial Community Characteristics. *Environ. Sci. Technol.* **2012**, *46* (19), 10579–10588.
(36) Zumstein, M. T.; Werner, J. J.; Helbling, D. E. Exploring the Specificity of Extracellular Wastewater Peptidases to Improve the Design of Sustainable Peptide-Based Antibiotics. *Environ. Sci. Technol.* **2020**, *54* (18), 11201–11209. https://doi.org/10.1021/acs.est.0c02564.
(37) Gulde, R.; Meier, U.; L. Schymanski, E.; E. Kohler, H.-P.; E. Helbling, D.; Derrer, S.; Rentsch, D.; Fenner, K. Systematic Exploration of Biotransformation Reactions of Amine-Containing Micropollutants in Activated Sludge. *Environ. Sci. Technol.* **2016**, *50* (6), 2908–2920. https://doi.org/10.1021/acs.est.5b05186.

(38) Rich, S.; Zumstein, M.; Helbling, D. Identifying Functional Groups That Determine Rates of Micropollutant Biotransformations Performed by Wastewater Microbial Communities. *Environ. Sci. Technol.* **2022**, *56* (2), 984–994. https://doi.org/10.1021/acs.est.1c06429.

(39) Prasse, C.; Wagner, M.; Schulz, R.; Ternes, T. A. Biotransformation of the Antiviral Drugs Acyclovir and Penciclovir in Activated Sludge Treatment. *Environ. Sci. Technol.* **2011**, *45* (7), 2761–2769. https://doi.org/10.1021/es103732y.

(40) Helbling, D. E.; Johnson, D. R.; Lee, T. K.; Scheidegger, A.; Fenner, K. A Framework for Establishing Predictive Relationships between Specific Bacterial 16S RRNA Sequence Abundances and Biotransformation Rates. *Water Res.* **2015**, *70*, 471–484. https://doi.org/10.1016/j.watres.2014.12.013.

(41) Wu, L.; Ning, D.; Zhang, B.; Li, Y.; Zhang, P.; Shan, X.; Zhang, Q.; Brown, M.; Li, Z.; Van Nostrand, J. D.; Ling, F.; Xiao, N.; Zhang, Y.; Vierheilig, J.; Wells, G. F.; Yang, Y.; Deng, Y.; Tu, Q.; Wang, A.; Acevedo, D.; Agullo-Barcelo, M.; Alvarez, P. J. J.; Alvarez-Cohen, L.; Andersen, G. L.; de Araujo, J. C.; Boehnke, K.; Bond, P.; Bott, C. B.; Bovio, P.; Brewster, R. K.; Bux, F.; Cabezas, A.; Cabrol, L.; Chen, S.; Criddle, C. S.; Deng, Y.; Etchebehere, C.; Ford, A.; Frigon, D.; Gómez, J. S.; Griffin, J. S.; Gu, A. Z.; Habagil, M.; Hale, L.; Hardeman, S. D.; Harmon, M.; Horn, H.; Hu, Z.; Jauffur, S.; Johnson, D. R.; Keller, J.; Keucken, A.; Kumari, S.; Leal, C. D.; Lebrun, L. A.; Lee, J.; Lee, M.; Lee, Z. M. P.; Li, Y.; Li, Z.; Li, M.; Li, X.; Ling, F.; Liu, Y.; Luthy, R. G.; Mendonça-Hagler, L. C.; de Menezes, F. G. R.; Meyers, A. J.; Mohebbi, A.; Nielsen, P. H.; Ning, D.; Oehmen, A.; Palmer, A.; Parameswaran, P.; Park, J.; Patsch, D.; Reginatto, V.; de los Reyes, F. L.; Rittmann, B. E.; Robles, A. N.; Rossetti, S.; Shan, X.; Sidhu, J.; Sloan, W. T.; Smith, K.; de Sousa, O. V.; Stahl, D. A.; Stephens, K.; Tian, R.; Tiedje, J. M.; Tooker, N. B.; Tu, Q.; Van Nostrand, J. D.; De los Cobos Vasconcelos, D.; Vierheilig, J.; Wagner, M.; Wakelin, S.; Wang, A.; Wang, B.; Weaver, J. E.; Wells, G. F.; West, S.; Wilmes, P.; Woo, S. G.; Wu, L.; Wu, J. H.; Wu, L.; Xi, C.; Xiao, N.; Xu, M.; Yan, T.; Yang, Y.; Yang, M.; Young, M.; Yue, H.; Zhang, B.; Zhang, P.; Zhang, Q.; Zhang, Y.; Zhang, T.; Zhang, Q.; Zhang, W.; Zhang, Y.; Zhou, H.; Zhou, J.; Wen, X.; Curtis, T. P.; He, Q.; He, Z.; Brown, M.; Zhang, T.; He, Z.; Keller, J.; Nielsen, P. H.; Alvarez, P. J. J.; Criddle, C. S.; Wagner, M.; Tiedje, J. M.; He, Q.; Curtis, T. P.; Stahl, D. A.; Alvarez-Cohen, L.; Rittmann, B. E.; Wen, X.; Zhou, J. Global Diversity and Biogeography of Bacterial Communities in Wastewater Treatment Plants. *Nat. Microbiol.* **2019**, *4* (July). https://doi.org/10.1038/s41564-019-0426-5.

(42) Wells, G. F.; Wu, C. H.; Piceno, Y. M.; Eggleston, B.; Brodie, E. L.; DeSantis, T. Z.; Andersen, G. L.; Hazen, T. C.; Francis, C. A.; Criddle, C. S. Microbial Biogeography across a Full-Scale Wastewater Treatment Plant Transect: Evidence for Immigration between Coupled Processes. *Appl. Microbiol. Biotechnol.* **2014**, *98* (10), 4723–4736. https://doi.org/10.1007/s00253-014-5564-3.

(43) Perrotta, A. R.; Kumaraswamy, R.; Bastidas-Oyanedel, J. R.; Alm, E. J.; Rodríguez, J. Inoculum Composition Determines Microbial Community and Function in an Anaerobic Sequential Batch Reactor. *PLoS One* **2017**, *12* (2). https://doi.org/10.1371/journal.pone.0171369.

(44) Polesel, F.; R. Andersen, H.; Trapp, S.; Gy. Plósz, B. Removal of Antibiotics in Biological Wastewater Treatment Systems—A Critical Assessment Using the Activated Sludge Modeling Framework for Xenobiotics (ASM-X). *Environ. Sci. Technol.* **2016**, *50* (19), 10316–10334. https://doi.org/10.1021/acs.est.6b01899.

(45) Jewell, K. S.; Castronovo, S.; Wick, A.; Falås, P.; Joss, A.; Ternes, T. A. New Insights into

the Transformation of Trimethoprim during Biological Wastewater Treatment. *Water Res.* **2016**, *88*, 550–557. https://doi.org/10.1016/J.WATRES.2015.10.026.
(46) Tian, R.; Posselt, M.; Fenner, K.; S. McLachlan, M. Increasing the Environmental Relevance of Biodegradation Testing by Focusing on Initial Biodegradation Kinetics and Employing Low-Level Spiking. *Environ. Sci. Technol. Lett.* **2022**, *10* (1), 40–45. https://doi.org/10.1021/acs.estlett.2c00811.
(47) Pochodylo, A. L.; Helbling, D. E. Emerging Investigators Series: Prioritization of Suspect Hits in a Sensitive Suspect Screening Workflow for Comprehensive Micropollutant Characterization in Environmental Samples. *Environ. Sci. Water Res. Technol.* **2017**, *3* (1), 54–65. https://doi.org/10.1039/C6EW00248J.
(48) Carpenter, C. M. G. G.; Wong, L. Y. J.; Johnson, C. A.; Helbling, D. E. Fall Creek Monitoring Station: Highly Resolved Temporal Sampling to Prioritize the Identification of Nontarget Micropollutants in a Small Stream. *Environ. Sci. Technol.* **2019**, *53* (1), 77–87. https://doi.org/10.1021/acs.est.8b05320.
(49) Kern, S.; Fenner, K.; Singer, H. P.; Schwarzenbach, R. P.; Hollender, J. Identification of Transformation Products of Organic Contaminants in Natural Waters by Computer-Aided Prediction and High-Resolution Mass Spectrometry. *Environ. Sci. Technol.* **2009**, *43* (18), 7039–7046. https://doi.org/10.1021/es901979h.
(50) Vogler, B. Development of a Comprehensive Multicomponent Screening Method for Polar Organic Compounds Using LC-Orbitrap. Improvement of the Solid Phase Extraction and Evaluation of Data Independent Acquisition, University of Zurich, 2013.
(51) Stravs, M. A.; Schymanski, E. L.; Singer, H. P.; Hollender, J. Automatic Recalibration and Processing of Tandem Mass Spectra Using Formula Annotation. *J. Mass Spectrom.* **2013**, *48* (1), 89–99. https://doi.org/10.1002/jms.3131.
(52) Ellis, L. B. M.; Gao, J.; Fenner, K.; Wackett, L. P. The University of Minnesota Pathway Prediction System: Predicting Metabolic Logic. *Nucleic Acids Res.* **2008**, *36* (Web Server issue), 427–432. https://doi.org/10.1093/nar/gkn315.
(53) Ellis, L. B.; Wackett, L. P. Use of the University of Minnesota Biocatalysis/Biodegradation Database for Study of Microbial Degradation. *Microb. Inform. Exp.* **2012**, *2* (1), 1–10. https://doi.org/10.1186/2042-5783-2-1.
(54) Wang, Y.; Fenner, K.; Helbling, D. E. Clustering Micropollutants Based on Initial Biotransformations for Improved Prediction of Micropollutant Removal during Conventional Activated Sludge Treatment. *Environ. Sci. Water Res. Technol.* **2020**, *6* (3), 554–565. https://doi.org/10.1039/c9ew00838a.
(55) Wicker, J.; Lorsbach, T.; Gütlein, M.; Schmid, E.; Latino, D.; Kramer, S.; Fenner, K. EnviPath - The Environmental Contaminant Biotransformation Pathway Resource. *Nucleic Acids Res.* **2016**, *44* (D1), D502–D508. https://doi.org/10.1093/nar/gkv1229.
(56) Murtagh, F.; Legendre, P. Ward's Hierarchical Agglomerative Clustering Method: Which Algorithms Implement Ward's Criterion? *J. Classif.* **2014**, *31* (3), 274–295. https://doi.org/10.1007/s00357-014-9161-z.
(57) The R Project for Statistical Computing https://www.r-project.org/.
(58) RStudio Team. RStudio: Integrated Development for R. http://www.rstudio.com/.
(59) Kolde, R. _pheatmap: Pretty Heatmaps_. https://cran.r-project.org/package=pheatmap.
(60) Jelic, A.; Gros, M.; Ginebreda, A.; Cespedes-Sánchez, R.; Ventura, F.; Petrovic, M.; Barcelo, D. Occurrence, Partition and Removal of Pharmaceuticals in Sewage Water and Sludge during Wastewater Treatment. *Water Res.* **2011**, *45* (3), 1165–1176.

https://doi.org/https://doi.org/10.1016/j.watres.2010.11.010.
(61) Paíga, P.; Correia, M.; Fernandes, M. J.; Silva, A.; Carvalho, M.; Vieira, J.; Jorge, S.; Silva, J. G.; Freire, C.; Delerue-Matos, C. Assessment of 83 Pharmaceuticals in WWTP Influent and Effluent Samples by UHPLC-MS/MS: Hourly Variation. *Sci. Total Environ.* **2019**, *648*, 582–600. https://doi.org/10.1016/J.SCITOTENV.2018.08.129.
(62) Zhi, H.; Webb, D. T.; Schnoor, J. L.; Kolpin, D. W.; Klaper, R. D.; Iwanowicz, L. R.; LeFevre, G. H. Modeling Risk Dynamics of Contaminants of Emerging Concern in a Temperate-Region Wastewater Effluent-Dominated Stream. *Environ. Sci. Water Res. Technol.* **2022**, *8* (7), 1408–1422. https://doi.org/10.1039/d2ew00157h.
(63) Vatovec, C.; Phillips, P.; Van Wagoner, E.; Scott, T. M.; Furlong, E. Investigating Dynamic Sources of Pharmaceuticals: Demographic and Seasonal Use Are More Important than down-the-Drain Disposal in Wastewater Effluent in a University City Setting. *Sci. Total Environ.* **2016**, *572*, 906–914. https://doi.org/10.1016/J.SCITOTENV.2016.07.199.
(64) Izabel-Shen, D.; Li, S.; Luo, T.; Wang, J.; Li, Y.; Sun, Q.; Yu, C.-P.; Hu, A. Repeated Introduction of Micropollutants Enhances Microbial Succession despite Stable Degradation Patterns. *ISME Commun.* **2022**, *2* (1). https://doi.org/10.1038/s43705-022-00129-0.
(65) Wolff, D.; Krah, D.; Dötsch, A.; Ghattas, A. K.; Wick, A.; Ternes, T. A. Insights into the Variability of Microbial Community Composition and Micropollutant Degradation in Diverse Biological Wastewater Treatment Systems. *Water Res.* **2018**, *143*, 313–324. https://doi.org/10.1016/J.WATRES.2018.06.033.
(66) Ju, F.; Zhang, T. Bacterial Assembly and Temporal Dynamics in Activated Sludge of a Full-Scale Municipal Wastewater Treatment Plant. *ISME J.* **2015**, *9* (3), 683–695. https://doi.org/10.1038/ismej.2014.162.
(67) Nguyen, J.; Lara-Gutiérrez, J.; Stocker, R. Environmental Fluctuations and Their Effects on Microbial Communities, Populations and Individuals. *FEMS Microbiology Reviews*. Oxford University Press July 1, 2021. https://doi.org/10.1093/femsre/fuaa068.
(68) Zhang, Y.; Zhao, Z.; Dai, M.; Jiao, N.; Herndl, G. J. Drivers Shaping the Diversity and Biogeography of Total and Active Bacterial Communities in the South China Sea. *Mol. Ecol.* **2014**, *23* (9), 2260–2274. https://doi.org/10.1111/mec.12739.
(69) Schymanski, E. L.; Jeon, J.; Gulde, R.; Fenner, K.; Ruff, M.; Singer, H. P.; Hollender, J. Identifying Small Molecules via High Resolution Mass Spectrometry: Communicating Confidence. *Environ. Sci. Technol.* **2014**, *48* (4), 2097–2098. https://doi.org/10.1021/es5002105.
(70) Wang, X.; Yu, N.; Yang, J.; Jin, L.; Guo, H.; Shi, W.; Zhang, X.; Yang, L.; Yu, H.; Wei, S. Suspect and Non-Target Screening of Pesticides and Pharmaceuticals Transformation Products in Wastewater Using QTOF-MS. *Environ. Int.* **2020**, *137*, 105599. https://doi.org/10.1016/J.ENVINT.2020.105599.
(71) Achermann, S.; Bianco, V.; Mansfeldt, C. B.; Vogler, B.; Kolvenbach, B. A.; Corvini, P. F. X.; Fenner, K. Biotransformation of Sulfonamide Antibiotics in Activated Sludge: The Formation of Pterin-Conjugates Leads to Sustained Risk. *Environ. Sci. Technol.* **2018**, *52* (11), 6265–6274. https://doi.org/10.1021/acs.est.7b06716.
(72) Funke, J.; Prasse, C.; Ternes, T. A. Identification of Transformation Products of Antiviral Drugs Formed during Biological Wastewater Treatment and Their Occurrence in the Urban Water Cycle. *Water Res.* **2016**, *98*, 75–83. https://doi.org/10.1016/J.WATRES.2016.03.045.
(73) Margot, J.; Rossi, L.; Barry, D. A.; Holliger, C. A Review of the Fate of Micropollutants in

780 Wastewater Treatment Plants. *Wiley Interdiscip. Rev. Water* **2015**, *2* (5), 457–487.
781 https://doi.org/10.1002/WAT2.1090.